

# METAL-INSULATOR TRANSITION IN HOMOGENEOUSLY DOPED GERMANIUM

MICHIO WATANABE

Department of Applied Physics and Physico-Informatics,  
Keio University, 3-14-1 Hiyoshi, Kohoku-ku,  
Yokohama 223-8522, Japan

## INTRODUCTION

The metal-insulator transition (MIT) in doped semiconductors with a random distribution of impurities is a unique quantum phase transition in the sense that both disorder and electron-electron interaction play a key role (see for example Refs. 1 and 2). The metallic phase of the transition is characterized by a finite electrical conductivity at  $T = 0$ , while the conductivity in the insulating phase vanishes in the limit of zero temperature. From a theoretical point of view, the correlation length in the metallic phase and the localization length in the insulating phase diverge at the critical point with the same exponent  $\nu$ , i.e., they are proportional to  $|N/N_c - 1|^{-\nu}$  in the critical regime of the MIT, and the value of  $\nu$  provides important information about the MIT. Here,  $N$  is the impurity concentration and  $N_c$  is the critical concentration for the MIT. Since direct experimental determination of  $\nu$  is extremely difficult, researchers have usually determined, instead of  $\nu$ , the value of the conductivity critical exponent  $\mu$  defined by

$$\sigma(0) = \sigma^*(N/N_c - 1)^\mu \quad (1)$$

immediately above  $N_c$  ( $0 < N/N_c - 1 \ll 1$ ). Here,  $\sigma(0)$  is the conductivity extrapolated to  $T = 0$  and  $\sigma^*$  is a prefactor. Values of  $\nu$  are then obtained assuming the relation  $\nu = \mu$  [3] which is valid for three-dimensional systems without electron-electron interaction. With a number of nominally uncompensated semiconductors  $\mu \approx 0.5$  has been obtained [2]. One of the best studied nominally uncompensated semiconductors is Si:P. Rosenbaum *et al.* studied both the doping-induced MIT and the uniaxial-stress-induced MIT, and showed that Eq. (1) describes  $\sigma(0)$  of Si:P with a single exponent  $\mu \approx 0.5$  over a wide range  $0.001 \leq N/N_c - 1 < 1$  [4]. Here, uniaxial stress was used for “tuning” because fine control of  $N/N_c - 1$  is difficult. In the same material, however,  $\mu \approx 1.3$  was claimed about ten years later for a narrow regime  $N_c < N < 1.1N_c$  by

a different group [5]. Moreover,  $\mu \approx 1$  was reported recently for the MIT driven by uniaxial stress [6]. As the origin of the discrepancy, inhomogeneous distribution of the impurities has been pointed out [7].

For the case of melt- (or metallurgically) doped samples, which have been employed in most of the previous studies including Refs. 4 – 6, the spatial fluctuation of  $N$  due to dopant striations and segregation can easily be on the order of 1% across a typical sample for the four-point resistance measurement that has a length of  $\sim 5$  mm or larger (see for example Ref. 8). For this reason, it will not be meaningful to discuss physical properties in the critical regime (e.g.,  $|N/N_c - 1| < 0.01$ ), unless one evaluates the macroscopic inhomogeneity in the samples and its influence on the results. In order to rule out the ambiguity arising from the inhomogeneity, we prepared  $^{70}\text{Ge}:\text{Ga}$  samples by neutron-transmutation doping (NTD) of isotopically enriched  $^{70}\text{Ge}$  single crystals. The NTD method inherently guarantees the random distribution of the dopants down to the atomic level [9,10]. We show from the conductivity measurements at  $T = 0.02 - 1$  K that  $\sigma(0)$  of the NTD  $^{70}\text{Ge}:\text{Ga}$  samples is described by Eq. (1) with  $\mu = 0.50 \pm 0.04$  over a wide range  $4 \times 10^{-4} \leq N/N_c - 1 < 0.4$  [11].

In order to determine  $\nu$  without assuming  $\mu = \nu$ , we have analyzed the temperature dependence of the conductivity on the insulating side of the MIT in the context of variable-range-hopping (VRH) conduction within the Coulomb gap [12]. Low-temperature ( $T < 0.5$  K) conductivity of the insulating  $^{70}\text{Ge}:\text{Ga}$  samples obeys  $\sigma(T) = \tilde{\sigma}(T) \exp[-(T_0/T)^{1/2}]$ , which is predicted by the VRH theory [13], with an appropriate temperature dependence in the prefactor  $\tilde{\sigma}(T)$ . Magnetic field and temperature dependence of the conductivity of the samples are subsequently measured in order to determine directly the localization length  $\xi$  and the impurity dielectric susceptibility  $\chi_{\text{imp}}$  as a function of  $N$  in the context of the theory. This kind of determination of  $\xi$  and  $\chi_{\text{imp}}$  was performed for compensated Ge:As by Ionov *et al.* [14] They found  $\xi \propto (1 - N/N_c)^{-\nu}$  and  $\chi_{\text{imp}} \propto (N_c/N - 1)^{-\zeta}$  with  $\nu = 0.60 \pm 0.04$  and  $\zeta = 1.38 \pm 0.07$ , respectively, for samples having  $N$  up to  $0.96N_c$ . The significance of their result is the experimental verification of the relation  $2\nu \approx \zeta$  that had been predicted by scaling theories [15]. However, the critical exponents of compensated samples are known to be different from those of nominally uncompensated samples [11]. Therefore, our determination of  $\xi$  and  $\chi_{\text{imp}}$  in nominally uncompensated samples is important.

The previous effort to measure the impurity dielectric susceptibility as a function of  $N$  has also contributed greatly. Hess *et al.* found  $\zeta = 1.15 \pm 0.15$  in nominally uncompensated Si:P [16]. Since  $\mu \approx 0.5$  was determined for the same series of Si:P samples [4], the relation  $2\mu \approx \zeta$  was again valid. Katsumoto has found  $\zeta \approx 2$  and  $\mu \approx 1$  for compensated  $\text{Al}_{0.3}\text{Ga}_{0.7}\text{As}:\text{Si}$ , i.e., again,  $2\mu \approx \zeta$  applies [17]. Thus, in these cases the conclusion  $2\nu \approx \zeta$  was reached indirectly, *by assuming*  $\mu = \nu$ . We, on the other hand, determine  $\nu$  directly, i.e., we do not have to rely on the assumption  $\mu = \nu$  in order to study the behavior of the localization length  $\xi$  near the MIT.

According to theories [2] on the MIT which take into account both disorder and electron-electron interaction, the critical exponents do not depend on the details of the system, but depend only on the universality class to which the system belongs. Moreover, there is an inequality  $\nu \geq 2/3$ , which is expected to apply generally to disordered systems irrespective of the presence of electron-electron interaction [18]. Hence, if one assumes  $\mu = \nu$ , which is derived for systems *without* electron-electron interaction,  $\mu \approx 0.5$  violates the inequality. This discrepancy has been known as the conductivity critical exponent puzzle. Kirkpatrick and Belitz have claimed that there are logarithmic corrections to scaling in universality classes with time-reversal symmetry, i.e., when the external magnetic field is zero, and that  $\mu \approx 0.5$ , found at  $B = 0$ , should be interpreted as an “effective” exponent which is different from a “real” exponent satisfying  $\mu \geq 2/3$  [19]. Therefore, comparison of  $\mu$  with and without the time-reversal symme-

try, i.e., with and without external magnetic fields becomes important. We study the MIT of  $^{70}\text{Ge}:\text{Ga}$  in magnetic fields up to  $B = 8$  T and show that  $\mu$  changes from 0.5 at  $B = 0$  to 1.1 at  $B \geq 4$  T [20]. The same exponent  $\mu' = 1.1$  is also found in the magnetic-field-tuned MIT for three different samples, i.e.,

$$\sigma(N, B, T \rightarrow 0) \propto [B_c(N) - B]^{\mu'}, \quad (2)$$

where  $B_c(N)$  is the critical magnetic field for concentration  $N$ . Moreover, an excellent finite-temperature scaling [2]

$$\sigma(N, B, T) \propto T^x f(|B_c(N) - B|/T^y), \quad (3)$$

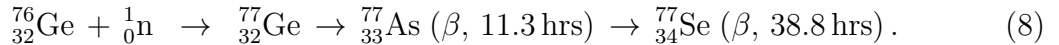
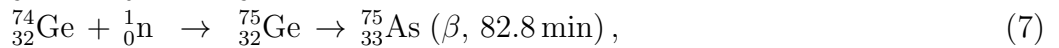
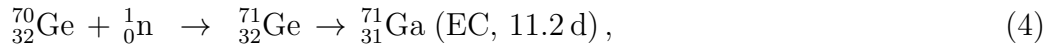
where  $x/y$  is equivalent to  $\mu'$ , is obtained with the same value of  $\mu'$ . The phase diagram on the  $(N, B)$  plane is successfully constructed, and we find a simple scaling rule which  $\sigma(N, B, T \rightarrow 0)$  would obey and derive from a simple mathematical argument that  $\mu = \mu'$  as has been observed in our experiment.

## EXPERIMENTS

### Sample preparation

All of the  $^{70}\text{Ge}:\text{Ga}$  samples were prepared by neutron-transmutation doping (NTD) of isotopically enriched  $^{70}\text{Ge}$  single crystals. The basic idea of NTD is as follows. Suppose that a nucleus in a crystal of a semiconductor captures a thermal neutron. After the capture, the nucleus is not necessarily stable. If it is stable, the element remains unchanged, but if it is not, it decays and transmutes into a new element which may act as a dopant. This is NTD. Practically, a crystal is placed in a nuclear reactor which produces thermal neutrons. Since the neutron field produced by a reactor is large enough to guarantee a homogeneous flux over the crystal dimensions and the small capture cross section (typically  $10^{-24}$  cm<sup>2</sup>) of semiconductors for neutrons minimizes “self-shadowing”, NTD is known to produce the most homogeneous, perfectly random distribution of dopant down to the atomic level [9].

As for Ge, there are five stable isotopes:  $^{70}\text{Ge}$  (20.5%),  $^{72}\text{Ge}$  (27.4%),  $^{73}\text{Ge}$  (7.8%),  $^{74}\text{Ge}$  (36.5%), and  $^{76}\text{Ge}$  (7.8%). The numbers in the parentheses represent the natural abundance. These five stable isotopes of Ge undergo the following nuclear reactions after capturing a thermal neutron.



Here,  ${}^1_0\text{n}$  is a neutron, EC and  $\beta$  denote electron capture and  $\beta$  decay, respectively, and the time in the parentheses represents the half life. Note that the natural Ge form both acceptors (Ga) and donors (As and Se) after NTD. Empirically, the impurity compensation is known to affect the value of the critical exponent [11]. To avoid the impurity compensation, we use isotopically enriched  $^{70}\text{Ge}$ .

The Czochralski grown, chemically very pure  $^{70}\text{Ge}$  crystal has isotopic composition  $[^{70}\text{Ge}] = 96.2$  at. % and  $[^{72}\text{Ge}] = 3.8$  at. % [10]. The as-grown crystal is free of dislocations,  $p$  type with a net electrically-active-impurity concentration less than  $5 \times 10^{11}$  cm<sup>-3</sup>. The thermal neutron irradiation was performed with the thermal to fast neutron ratio of

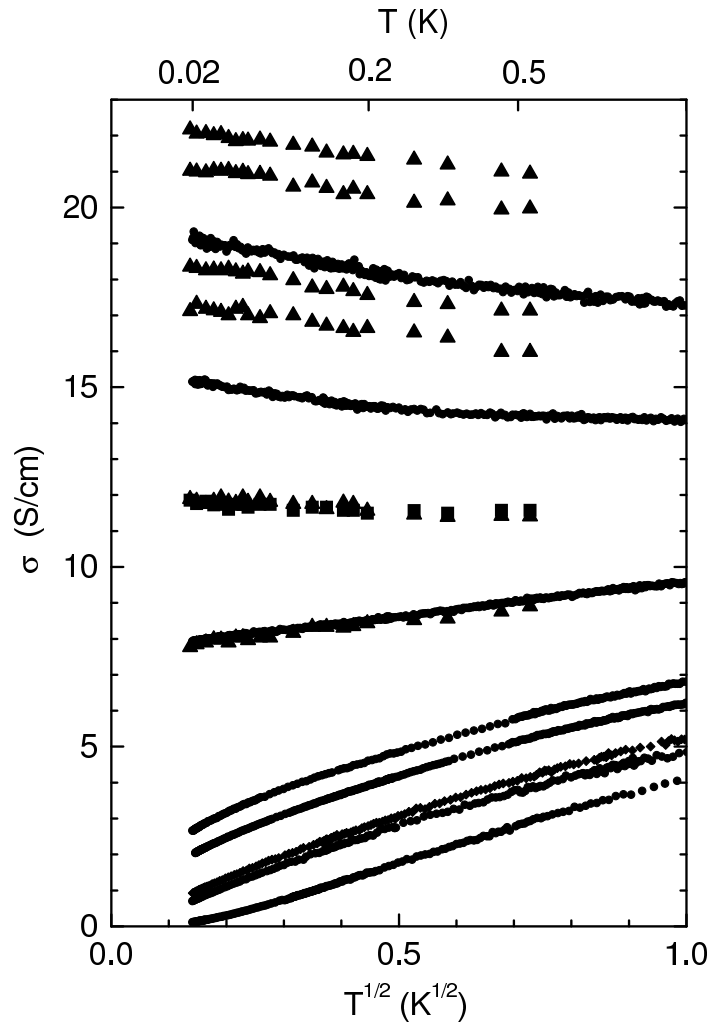


**Figure 1.** Electrical conductivity as a function of  $T^{1/2}$  for NTD  $^{70}\text{Ge}:\text{Ga}$ . From bottom to top in units of  $10^{17} \text{ cm}^{-3}$ , the Ga concentrations are 1.853, 1.856, 1.858, 1.861, 1.863, 1.912, 1.933, 2.004, 2.076, 2.210, 2.219, 2.232, 2.290, 2.362, and 2.434, respectively.

$\approx 30:1$ . The small fraction of  $^{72}\text{Ge}$  becomes  $^{73}\text{Ge}$  which is stable, i.e., no further acceptors or donors are introduced. The post-NTD rapid thermal annealing at  $650^\circ\text{C}$  for 10 sec removed most of the irradiation-induced defects from the samples. The short annealing time is important in order to avoid the redistribution and/or clustering of the uniformly dispersed  $^{71}\text{Ga}$  acceptors. The concentration of the electrically active radiation defects measured with deep level transient spectrometry (DLTS) after the annealing is less than 0.1% of the Ga concentration, i.e., the compensation ratio of the samples is less than 0.001. The dimension of most samples used for conductivity measurements was  $6 \times 0.9 \times 0.7 \text{ mm}^3$ . Four strips of boron-ion-implanted regions on a  $6 \times 0.9 \text{ mm}^2$  face of each sample were coated with 200 nm Pd and 400 nm Au pads using a sputtering technique. Annealing at  $300^\circ\text{C}$  for one hour activated the implanted boron and removed the stress in the metal films.

The concentration of Ga acceptors after NTD is determined from the time of thermal-neutron irradiation. The concentration is proportional to the irradiation time as long as the same irradiation site and the same power of a nuclear reactor are employed.

## Low-temperature measurements

The electrical conductivity measurements were carried out down to temperatures of 20 mK using a  $^3\text{He}$ - $^4\text{He}$  dilution refrigerator. All the electrical leads were low-pass filtered at the top of the cryostat. The sample was fixed in the mixing chamber and a ruthenium oxide thermometer [Scientific Instrument (SI), RO600A,  $1.4 \times 1.3 \times 0.5 \text{ mm}^3$ ] was placed close to the sample. To measure the resistance of the thermometer, we used an ac resistance bridge (RV-Elekroniikka, AVS-47). The thermometer was calibrated against  $2\text{Ce}(\text{NO}_3)_3 \cdot 3\text{Mg}(\text{NO}_3)_2 \cdot 24\text{H}_2\text{O}$  (CMN) susceptibility and against the resistance of a canned ruthenium oxide thermometer (SI, RO600A2) which was calibrated commercially over a temperature range from 50 mK to 20 K. We employed an ac method at 21.0 Hz to measure the resistance of the sample. The power dissipation was kept below  $10^{-14}$  W, which is small enough to avoid overheating of the samples. The output voltage of the sample was detected by a lock-in amplifier (EG&G Princeton Applied Research, 124A). All the analog instruments as well as the cryostat were placed inside a shielded room. The output of the instruments was detected by digital voltmeters placed outside the shielded room. All the electrical leads into the shielded room were low-pass filtered. The output of the voltmeters was read by a personal computer via GP-IB interface connected through an optical fiber. Magnetic fields up to 8 T were applied in the direction perpendicular to the current flow by means of a superconducting solenoid.

## RESULTS AND DISCUSSION

### Temperature dependence of conductivity in metallic samples and the critical exponent for the zero-temperature conductivity

The temperature dependence of the electrical conductivity mostly for the metallic samples is shown in Fig. 1. The temperature variation of the conductivity of disordered metal is governed mainly by electron-electron interaction at low temperatures [1], and can be written as

$$\Delta\sigma(T) \equiv \sigma(T) - \sigma(0) = m\sqrt{T}, \quad (9)$$

where

$$m = \frac{e^2}{\hbar} \frac{1}{4\pi^2} \frac{1.3}{\sqrt{2}} \left( \frac{4}{3} - \frac{3}{2} \tilde{F} \right) \sqrt{\frac{k_B}{\hbar D}} = A/\sqrt{D}. \quad (10)$$

Here,  $\tilde{F}$  is a dimensionless and temperature-independent parameter characterizing the Hartree interaction and  $D$  is the diffusion constant [1], which is related to the conductivity via the Einstein relation

$$\sigma = (\partial n / \partial \mu) e^2 D, \quad (11)$$

where  $(\partial n / \partial \mu)$  is the density of states at the Fermi level. In various reports such as Refs. 5 and 10,  $\sigma(0)$  was obtained by extrapolating  $\sigma(T)$  to  $T = 0$  assuming  $\sqrt{T}$  dependence based on Eq. (9). One should note, however, that it is sound only in the limit of  $\Delta\sigma(T) \ll \sigma(0) \approx \sigma(T)$ , where  $D$  can be considered as a constant, i.e.,  $m$  is constant, and that the inequality is no longer valid as  $N$  approaches  $N_c$  from the metallic side since  $\sigma(0)$  also approaches zero. In such cases  $m$  in Eq. (9) is not temperature independent and  $\Delta\sigma(T)$  may exhibit a temperature dependence different from  $\sqrt{T}$ . To examine this point in our experimental results, we go back to Fig. 1. We see there that  $\Delta\sigma(T)$  of the bottom five curves are not proportional to  $\sqrt{T}$ , while  $\Delta\sigma(T)$  of the other higher  $N$  samples are described by  $\propto \sqrt{T}$ . The close-ups of  $\sigma(T)$  for the six samples with positive  $d\sigma/dT$  in the scale of  $\sqrt{T}$  and  $T^{1/3}$  are shown in Figs. 2(a)

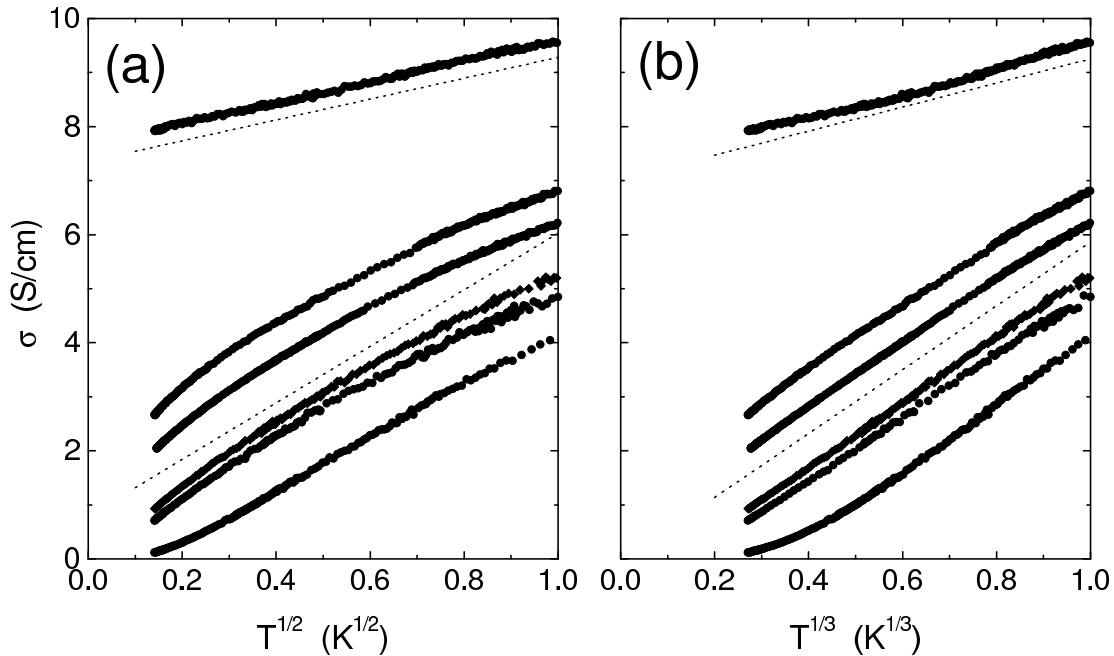


**Figure 2.** Conductivity as a function of (a)  $T^{1/2}$  and (b)  $T^{1/3}$ , respectively, near the metal-insulator transition. From bottom to top in units of  $10^{17} \text{ cm}^{-3}$ , the concentrations are 1.853, 1.856, 1.858, 1.861, 1.863, and 1.912, respectively. The upper and lower dotted lines in each figure represent the best fit using the data between 0.05 K and 0.5 K for the first and the third curves from the top, respectively. Each fit is shifted downward slightly for easier comparison.

and 2(b), respectively. The upper and lower dotted lines represent the best fit using the data between 0.05 K and 0.5 K for the samples with  $N = 1.912 \times 10^{17} \text{ cm}^{-3}$  and  $N = 1.861 \times 10^{17} \text{ cm}^{-3}$ , respectively. Each fit is shifted downward slightly for the sake of clarity. From this comparison, it is clear that a  $T^{1/3}$  dependence rather than a  $\sqrt{T}$  dependence holds for samples in the very vicinity of the MIT. The opposite is true for the curve at the top. This means that the  $\sqrt{T}$  dependence in Eq. (9) is replaced by a  $T^{1/3}$  dependence as the MIT is approached.

A  $T^{1/3}$  dependence close to the critical point for the MIT was predicted originally by Al'tshuler and Aronov [21]. They considered an interacting electron system with paramagnetic impurities, for which they obtained a single parameter scaling equation. At finite temperatures, they assumed a scaling form for conductivity according to the scaling hypothesis:

$$\sigma = \frac{e^2}{\hbar \xi'} f_1(\xi'/L_T), \quad (12)$$

where  $\xi'$  is the correlation length and  $L_T \equiv \sqrt{\hbar D/k_B T}$  is the thermal diffusion length. When  $L_T \gg \xi'$ ,  $f_1(\xi'/L_T) = A_0 + A_1 \xi'/L_T$ , which is equivalent to Eq. (9). In the critical region, where  $L_T \ll \xi' \rightarrow \infty$ , Eq. (12) should be reduced to

$$\sigma = C_1 \frac{e^2}{\hbar L_T}. \quad (13)$$

Combining this equation and Eq. (11), they obtained  $\sigma \propto T^{1/3}$ . The  $T^{1/3}$  dependence was also predicted from numerical calculations that consider solely the effect of disorder [22].

It is not clear whether the argument in Refs. 21 or 22 is applicable to the present system or not, but there is an experimental fact that  $\sqrt{T}$  dependence of conductivity

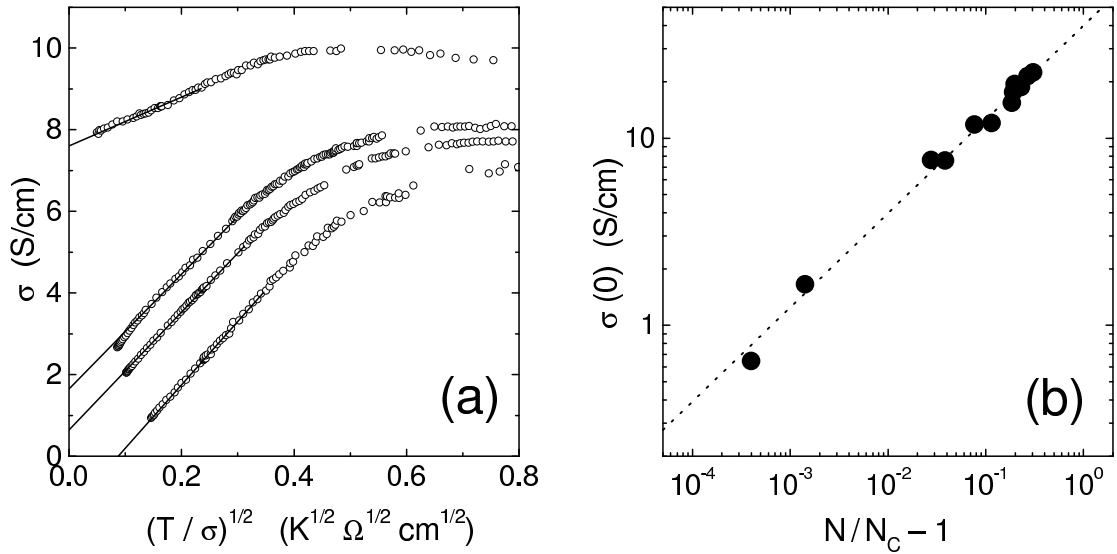


**Figure 3.** (a) Conductivity  $\sigma$  as a function of  $(T/\sigma)^{1/2}$ . From bottom to top in units of  $10^{17} cm^{-3}$ , the concentrations are 1.858, 1.861, 1.863, and 1.912, respectively. The solid lines denote the extrapolation for finding  $\sigma(0)$ . (b) Zero-temperature conductivity  $\sigma(0)$  vs the dimensionless distance  $N/N_c - 1$  from the critical point on a double logarithmic scale. The dotted line represents the best power-law fit by  $\sigma(0) \propto (N/N_c - 1)^\mu$  where  $\mu = 0.50 \pm 0.04$ .

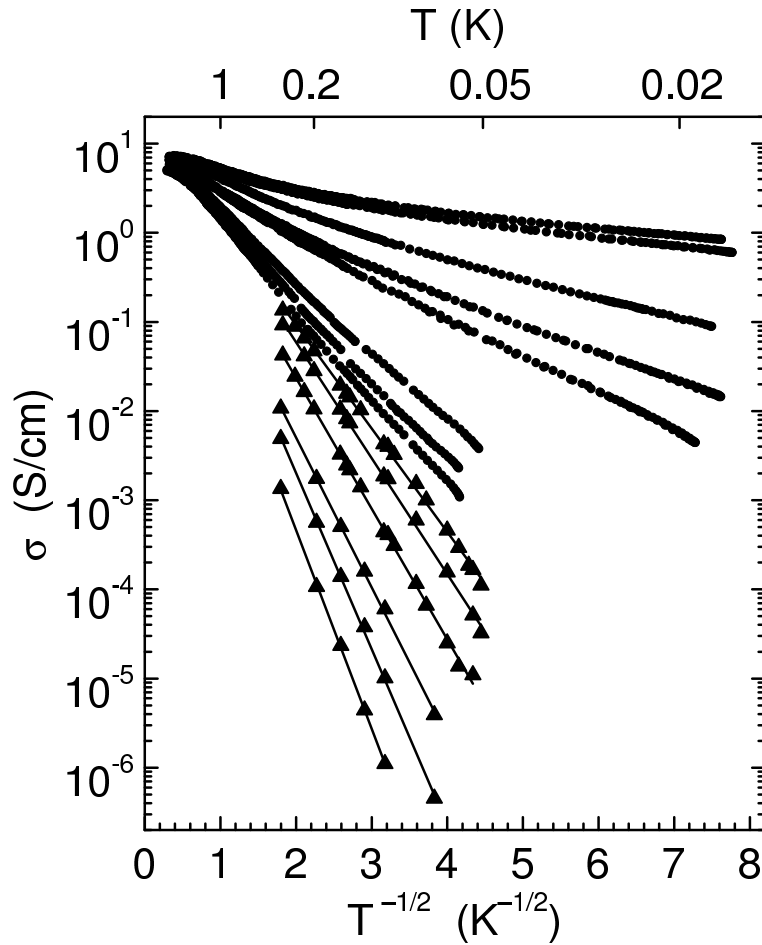


**Figure 4.** The logarithm of the conductivity as a function of  $T^{-1/2}$  for insulating samples. the concentrations from bottom to top in units of  $10^{17} cm^{-3}$  are 1.717, 1.752, 1.779, 1.796, 1.805, 1.823, 1.840, 1.842, 1.843, 1.848, 1.850, 1.853, 1.856, and 1.858, respectively.

changes to  $T^{1/3}$  as  $N_c$  is approached. It is important that we find a consistent method that allows the determination of  $\sigma(0)$  for both the cases. For this purpose, we follow Al'tshuler and Aronov's manipulation [21] of eliminating  $m$  and  $D$  in Eqs. (9)–(11) and obtain

$$\sigma(T) = \sigma(0) + m' \sqrt{T/\sigma(T)}, \quad (14)$$

where  $m' = eA\sqrt{(\partial n/\partial \mu)}$ , which is temperature independent. In the limit of  $\Delta\sigma(T) \ll \sigma(0) \approx \sigma(T)$ , this equation gives the same value of  $\sigma(0)$  as Eq. (9) does. When  $\sigma(0) \ll \sigma(T)$ , it yields a  $T^{1/3}$  dependence for  $\sigma(T)$ . Thus, it is applicable to both  $\sqrt{T}$  and  $T^{1/3}$  dependent conductivity. From today's theoretical understanding of the problem, Eqs. (9) and (14) are valid only for  $L_T \gg \xi'$ , and their applicability to the critical region is not clear, because the higher-order terms of the  $\beta$  function [23] which were once erroneously believed to be zero do not vanish [24]. Nevertheless, we expect Eq. (14) to be a good expression for describing the temperature dependence of all metallic samples because it expresses both  $\sqrt{T}$  and  $T^{1/3}$  dependences as limiting forms. Then, based on Eq. (14), we plot  $\sigma(T)$  vs  $\sqrt{T/\sigma(T)}$  for the four close to  $N_c$  samples in Fig. 3(a). The data points align on straight lines, which supports the adequacy of Eq. (14). The zero-temperature conductivity  $\sigma(0)$  is obtained by extrapolating to  $T = 0$ . The curve on the top of Fig. 3(a) is for the sample with the lowest  $N$  among the ones showing  $\sqrt{T}$  dependence at low temperatures, i.e., this sample has the largest value of  $\Delta\sigma(T)/\sigma(0)$  among  $\sqrt{T}$  samples. The value of  $\sigma(0)$  obtained for this particular sample using Eq. (14) differs only by 0.6% from the value determined by the conventional extrapolation assuming Eq. (9). This small difference is comparable to the variation arising from the choice of the temperature range in which the fitting is performed. Therefore, the extrapolation method proposed here is compatible with the conventional method based on the  $\propto \sqrt{T}$  extrapolation.

Based on this analysis the MIT is found to occur between the first and second samples from the bottom in Fig. 3(a), i.e.,  $1.858 \times 10^{17} \text{ cm}^{-3} < N_c < 1.861 \times 10^{17} \text{ cm}^{-3}$ . Thus, unlike the case for Si:P [5,7],  $N_c$  is fixed already within an accuracy of 0.16% and the evaluation of the critical exponent  $\mu$  will *not* be affected by the ambiguity in the determination of  $N_c$ . Figure 3(b) shows the zero-temperature conductivity  $\sigma(0)$  as a function of  $N/N_c - 1$  on a double logarithmic scale. A fit of Eq. (1) (dotted line) is excellent all the way down to  $(N/N_c - 1) = 4 \times 10^{-4}$ . The fitting parameters are  $\mu = 0.50 \pm 0.04$ ,  $N_c = (1.860 \pm 0.002) \times 10^{17} \text{ cm}^{-3}$ , and  $\sigma^* = (40 \pm 2) \text{ S/cm}$ . We note that  $\mu = 0.46 \pm 0.18$  is obtained even when we use only the four samples closest to  $N_c$  for the fitting.

### Variable-range-hopping conduction in insulating samples and the critical exponents for localization length and dielectric susceptibility

The temperature dependence of the conductivity  $\sigma(T)$  of insulating samples is shown in Fig. 4. The electrical conduction of doped semiconductors on the insulating side of the MIT is often dominated by variable-range hopping (VRH) at low temperatures. The temperature dependence of  $\sigma(T)$  for VRH is written in the form of

$$\sigma(T) = \tilde{\sigma}(T) \exp[-(T_0/T)^p], \quad (15)$$

where  $p = 1/2$  for the excitation within a parabolic-shaped energy gap (Coulomb gap), and  $p = 1/4$  for a constant single-particle density of states around the Fermi level [13]. The temperature dependence of  $\tilde{\sigma}(T)$  contributes greatly to the temperature dependence of  $\sigma(T)$  near  $N_c$  because the factor  $T_0/T$  in the exponential term becomes very small, i.e., the temperature dependencies of the prefactor and that of the exponential

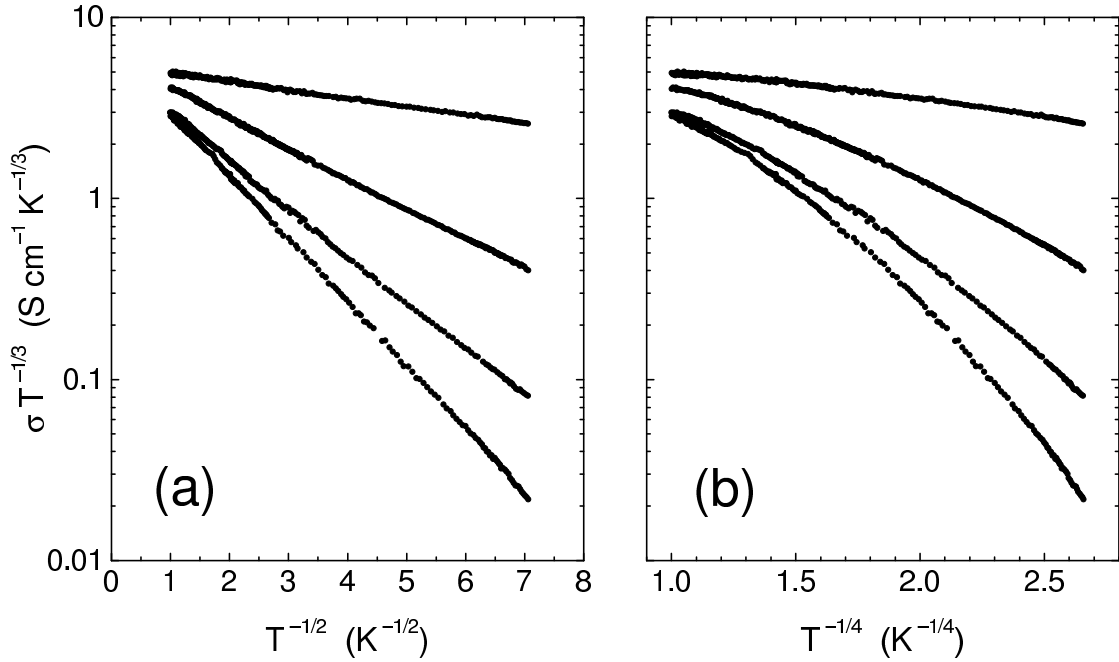


**Figure 5.** Conductivity multiplied by  $T^{-1/3}$  vs (a)  $T^{-1/2}$  and (b)  $T^{-1/4}$ . From bottom to top in units of  $10^{17} \text{ cm}^{-3}$ , the concentrations are 1.848, 1.850, 1.853, and 1.856, respectively.

term become comparable. Theoretically,  $\tilde{\sigma}(T)$  is expected to depend on temperature as

$$\tilde{\sigma}(T) \propto T^r \quad (16)$$

but the value of  $r$  including the sign has not been derived yet for VRH conduction with both  $p = 1/2$  and  $p = 1/4$ .

As we have seen in Fig. 2(b), the temperature variation of the low-temperature conductivity of the  $^{70}\text{Ge}:\text{Ga}$  samples within  $\pm 0.3\%$  of  $N_c$  is proportional to  $T^{1/3}$ . Since both the  $T^{1/3}$  dependence of the conductivity and the VRH with  $p = 1/2$  are results of the electron-electron interaction in disordered systems, they can be expressed, in principle, in a unified form. Moreover, the electronic transport in barely metallic samples and that in barely insulating samples should be essentially the same at high temperatures so long as the inelastic scattering length and the thermal diffusion length are smaller than, or at most comparable to the correlation length or the localization length. So, the temperature dependence of conductivity at high temperatures should be the same on both sides of the transition. Such behavior is confirmed experimentally in the present system, i.e., as seen in Fig. 2(b) the conductivity of samples very close to  $N_c$  shows a  $T^{1/3}$  dependence at  $T \approx 0.5 \text{ K}$ , irrespective of the phase (metal or insulator) to which they belong at  $T = 0$ . Based on this consideration we fix  $r = 1/3$ . Figure 5 shows  $\sigma T^{-r}$  with  $r = 1/3$  for four samples ( $N/N_c = 0.993, 0.994, 0.996,$  and  $0.998$ ) as a function of (a)  $T^{-1/2}$  and (b)  $T^{-1/4}$ . All the data points lie on straight lines with  $p = 1/2$  in Fig. 5(a) while they curve downward with  $p = 1/4$  in Fig. 5(b). This dependence is maintained even when we change the values of  $r$  between  $r = 1/2$  and  $1/4$ . Thus we conclude that the conductivity of all samples on the insulating side for  $N$  up to  $0.998N_c$  is described by the theory for the VRH conduction where the excitation occurs within the Coulomb gap, i.e., Eq. (15) with  $p = 1/2$ .

Based on these findings, we evaluate the  $N$  dependence of  $T_0$  in Eq. (15) with  $p = 1/2$  and  $r = 1/3$ . Figure 6 shows  $T_0$  as a function of  $1 - N/N_c$ . The vertical and horizontal error bars have been estimated based on the values of  $T_0$  obtained with  $r = 1/2$  and  $r = 1/4$ , and the values of  $1 - N/(1.858 \times 10^{17} \text{ cm}^{-3})$  and  $1 - N/(1.861 \times 10^{17} \text{ cm}^{-3})$ , where  $1.858 \times 10^{17} \text{ cm}^{-3}$  is the highest concentration in the insulating phase

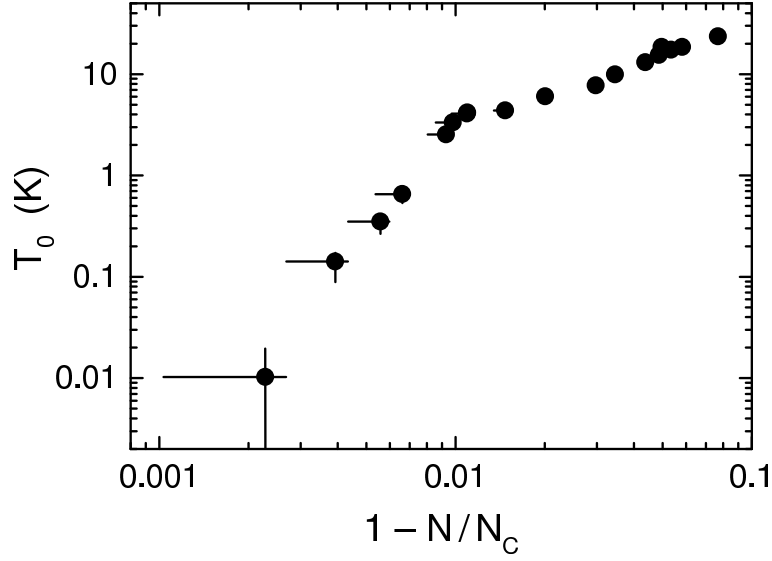


**Figure 6.**  $T_0$  determined by  $\sigma(T) \propto T^{1/3} \exp[-(T_0/T)^{1/2}]$  as a function of the dimensionless concentration  $1 - N/N_c$ .

and  $1.861 \times 10^{17} \text{ cm}^{-3}$  is the lowest in the metallic phase, respectively. According to theory [13],  $T_0$  in Eq. (15) is given by

$$k_B T_0 \approx \frac{1}{4\pi\epsilon_0} \frac{2.8e^2}{\epsilon(N)\xi(N)} \quad (17)$$

in SI units, where  $\epsilon(N)$  is the dielectric constant, and  $\xi(N)$  is the localization length. Here, we should note that the condition  $T < T_0$  is needed for the VRH theory to be valid, i.e.,  $T_0$  has to be evaluated only from the data obtained at temperatures low enough to satisfy the above condition. This requirement is fulfilled in Fig. 6 for all the samples except for the one with  $N = 0.998N_c$ . Concerning this latter sample, we will include it for the determination of  $\gamma$  (Fig. 8) and  $\xi$  and  $\chi_{\text{imp}}$  (Fig. 9) but not for the calculation of the critical exponents.

Our next step is to separate  $T_0$  into  $\epsilon$  and  $\xi$  in the framework of the theory of VRH conduction with and without a weak magnetic field [13]. For  $\xi/\lambda \ll 1$ , the magnetoconductance is expressed as

$$-\ln \left[ \frac{\sigma(B, T)}{\sigma(0, T)} \right] \approx 0.0015 \left( \frac{\xi}{\lambda} \right)^4 \left( \frac{T_0}{T} \right)^{3/2}, \quad (18)$$

where  $\lambda \equiv \sqrt{\hbar/eB}$  is the magnetic length in SI units. According to Eq. (18), the magnetic-field variation of  $\ln \sigma$  at  $T = \text{const.}$  is proportional to  $B^2$ , i.e.,

$$-\ln \sigma(B, T) = -\ln \sigma(0, T) + C_2(T)B^2, \quad (19)$$

and the slope  $C_2(T)$  in the above equation is proportional to  $T^{-3/2}$ . In order to demonstrate that these relations hold for our samples, we show for the  $N = 0.989N_c$  sample  $-\ln \sigma(B, T)$  vs  $B^2$  in Fig. 7(a) and  $C_2(T)$  determined by least-square fitting of  $-\partial \ln \sigma / \partial B^2$  vs  $T^{-3/2}$  in Fig. 7(b). Since Eq. (18) is equivalent to

$$\gamma \equiv C_2(T)/T^{-3/2} \approx 0.0015 (e/\hbar)^2 \xi^4 T_0^{3/2}, \quad (20)$$

$\xi$  is given by

$$\xi \approx 5.1 (\hbar/e)^{1/2} \gamma^{1/4} T_0^{-3/8}. \quad (21)$$

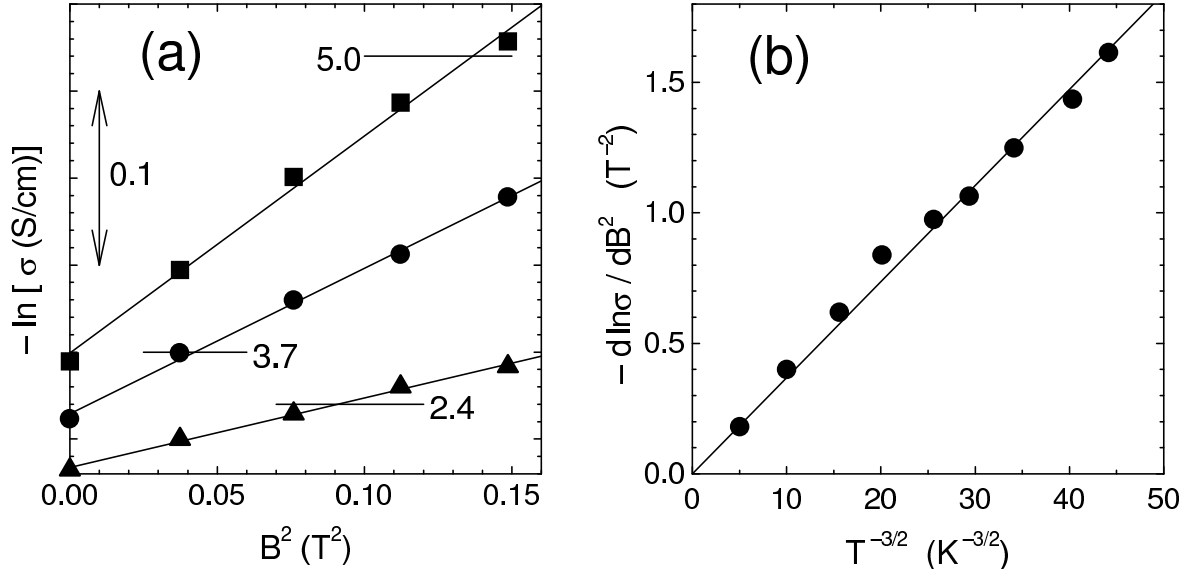


**Figure 7.** (a) Logarithm of  $\sigma^{-1}$  vs  $B^2$  at constant temperatures for the sample having  $N = 1.840 \times 10^{17} \text{ cm}^{-3}$ . From top to bottom the temperatures are 0.095 K, 0.135 K, and 0.215 K, respectively. The solid lines represent the best fits. (b) Slope  $-d \ln \sigma / dB^2$  vs  $T^{-3/2}$  for the same sample. The solid line represents the best fit.

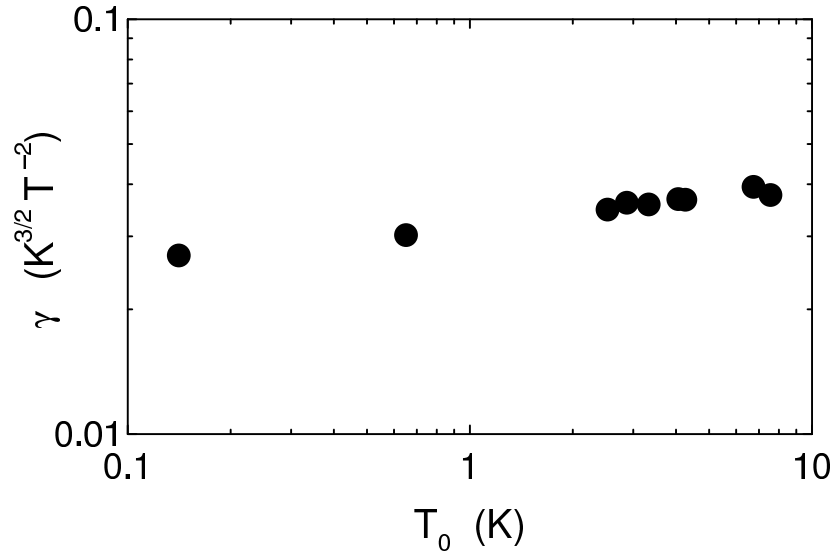


**Figure 8.** Coefficient  $\gamma$  defined by Eq. (20) as a function of  $T_0$ .

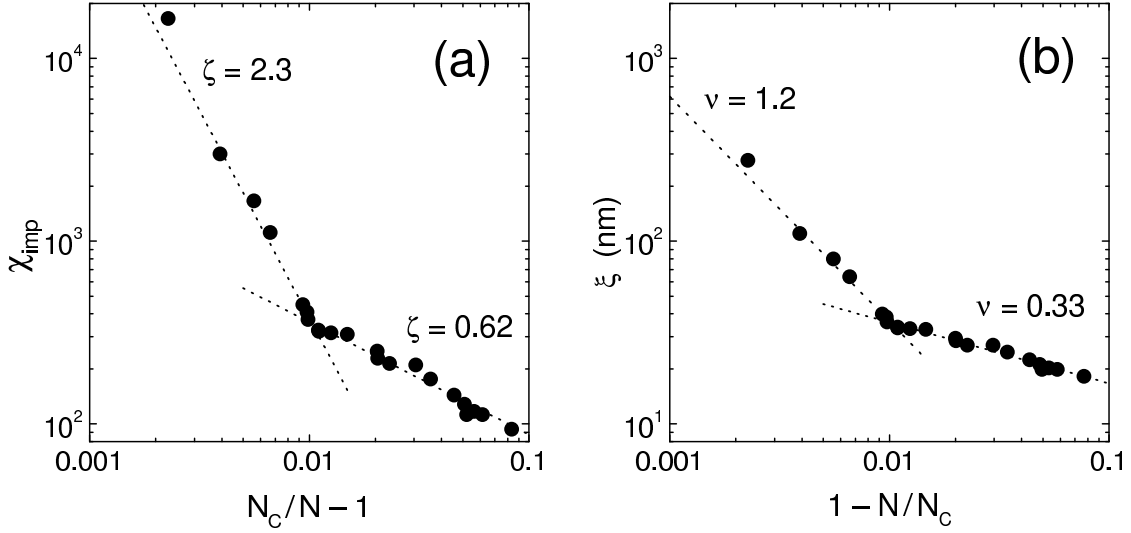


**Figure 9.** (a) Dielectric susceptibility  $\chi_{\text{imp}}$  arising from the impurities vs  $N_c/N - 1$ . (b) Localization length  $\xi$  vs  $1 - N/N_c$ .

In this way we have determined  $\gamma$  as a function of  $T_0$  for nine samples (Fig. 8). The value of  $\gamma$  is almost independent of  $T_0$ , and if one assumes the form of  $\gamma \propto T_0^\delta$ , one obtains a small value of  $\delta = 0.094 \pm 0.005$  from least-square fitting. We determine  $\xi$  and  $\chi_{\text{imp}} = \epsilon - \epsilon_h$  from Eqs. (17) and (21), and show them in Fig. 9 as a function of  $1 - N/N_c$  and  $N_c/N - 1$ , respectively. Here,  $\epsilon_h$  is the dielectric constant of the host Ge, and hence,  $\chi_{\text{imp}}$  is the dielectric susceptibility of the Ga acceptors. We should note that both  $\xi$  and  $\chi_{\text{imp}}$  are sufficiently larger than the Bohr radius (8 nm for Ge) and  $\epsilon_h = 15.4$  [25], respectively. According to the theories of the MIT, both  $\xi$  and  $\chi_{\text{imp}}$  diverge at  $N_c$  as  $\xi(N) \propto (1 - N/N_c)^{-\nu}$  and  $\chi_{\text{imp}}(N) \propto (N_c/N - 1)^{-\zeta}$ , respectively. We find, however, both  $\xi$  and  $\chi_{\text{imp}}$  do not show such simple dependencies on  $N$  in the range shown in Fig. 9, and that there is a sharp change of both dependencies at  $N \approx 0.99N_c$ . On both sides of the change in slope, the concentration dependence of  $\xi$  and  $\chi_{\text{imp}}$  are expressed well by the scaling formula as shown in Fig. 9. Theoretically, the quantities should show the critical behavior when  $N$  is very close to  $N_c$ . So  $\nu = 1.2 \pm 0.3$  and  $\zeta = 2.3 \pm 0.6$  may be concluded from the data in  $0.99 < N/N_c$ . However, the other region ( $0.9 < N/N_c < 0.99$ ), where we obtain  $\nu = 0.33 \pm 0.03$  and  $\zeta = 0.62 \pm 0.05$ , is also very close to  $N_c$  in a conventional experimental sense.

As a possible origin for the change in slope, we refer to the effect of compensation. Although our samples are nominally uncompensated, doping compensation of less than 0.1% may be present due to residual isotopes that become  $n$ -type impurities after NTD. In addition to the doping compensation, the effect known as “self compensation” may play an important role near  $N_c$  [26]. It is empirically known that the doping compensation affects the value of the critical exponents [11]. Rentzsch *et al.* studied VRH conduction of  $n$ -type NTD Ge in the concentration range of  $0.2 < N/N_c < 0.91$ , and showed that  $T_0$  vanishes as  $T_0 \propto (1 - N/N_c)^\alpha$  with  $\alpha \approx 3$  for  $K = 38\%$  and  $54\%$ , where  $K$  is the compensation ratio [27]. Since  $\alpha \approx \nu + \zeta$  [Eq. (17)], we find for our NTD  $^{70}\text{Ge}:\text{Ga}$  samples  $\alpha = 3.5 \pm 0.8$  for  $0.99 < N/N_c < 1$  and  $\alpha = 0.95 \pm 0.08$  for  $0.9 < N/N_c < 0.99$ . Interestingly,  $\alpha = 3.5 \pm 0.8$  agrees with  $\alpha \approx 3$  found for compensated samples. Moreover, we have recently proposed the possibility that the conductivity critical exponent  $\mu \approx 1$  in the same  $^{70}\text{Ge}:\text{Ga}$  only within the very vicinity of  $N_c$  (up to about +0.1% of  $N_c$ ) [28]. An exponent of  $\mu = 0.50 \pm 0.04$ , on the other hand, holds for a wider region of  $N$  up to  $1.4N_c$  as we have seen in Fig. 3(b). Again,  $\mu \approx 1$  near  $N_c$  may be viewed as the effect of compensation. Therefore, it may be

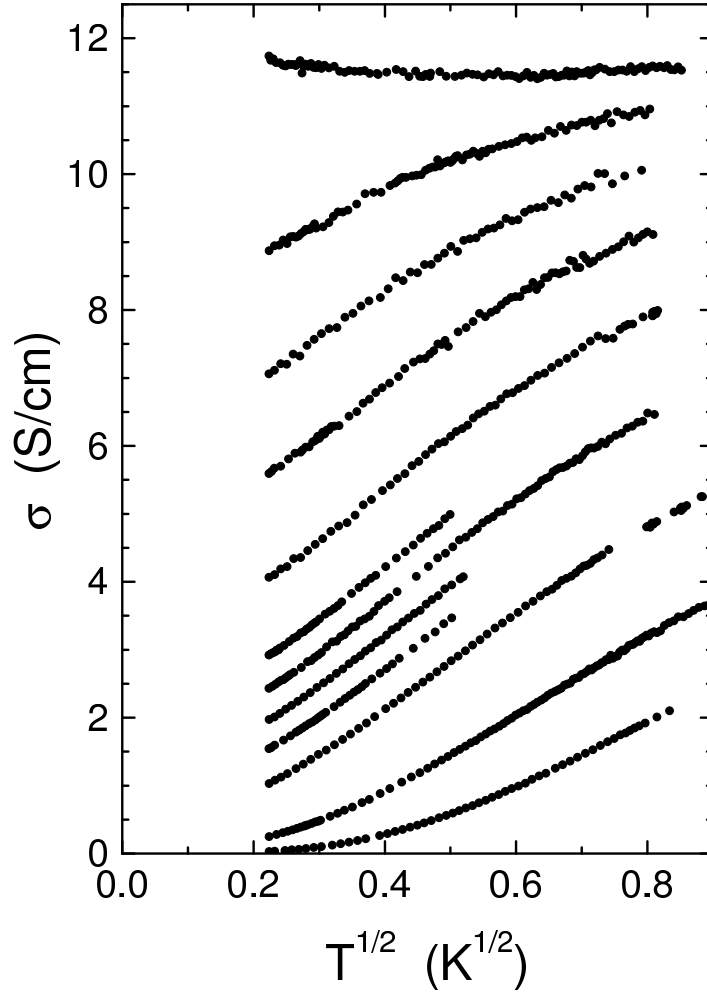


**Figure 10.** Conductivity of the sample having  $N = 2.004 \times 10^{17} \text{ cm}^{-3}$  as a function of  $T^{1/2}$  at several magnetic fields. The values of the magnetic induction from top to bottom in units of tesla are 0.0, 1.0, 2.0, 3.0, 4.0, 4.7, 5.0, 5.3, 5.6, 6.0, 7.0, and 8.0, respectively.

possible that the region of  $N$  around  $N_c$  where  $\nu \approx 1$  and  $\mu \approx 1$  changes its width as a function of the doping compensation. In the limit of zero compensation, the part which is characterized by  $\nu \approx 1$  and  $\mu \approx 1$  vanishes, i.e., we propose  $\nu = 0.33 \pm 0.03$ ,  $\zeta = 0.62 \pm 0.05$ , and  $\mu = 0.50 \pm 0.04$  for truly uncompensated systems and that the relation  $\mu = \nu$  [3] is not satisfied. In compensated systems, on the other hand,  $\mu = \nu$  may hold as it does in the very vicinity of  $N_c$ . However, the preceding discussion needs to be proven experimentally in the future by using samples whose compensation ratios are controlled precisely and systematically.

### Metal-insulator transition in magnetic fields

Figure 10 shows the temperature dependence of the conductivity of the sample having  $N = 2.004 \times 10^{17} \text{ cm}^{-3}$  for several values of the magnetic induction  $B$ . Application of the magnetic field decreases the conductivity and eventually drives the sample into the insulating phase. This property can be understood in terms of the shrinkage of the wave function due to the magnetic field. In strong magnetic fields and at low temperatures, i.e., when  $g\mu_B B \gg k_B T$ , the conductivity shows another  $\sqrt{T}$  dependence [1]

$$\sigma(N, B, T) = \sigma(N, B, 0) + m_B(N, B) \sqrt{T}, \quad (22)$$

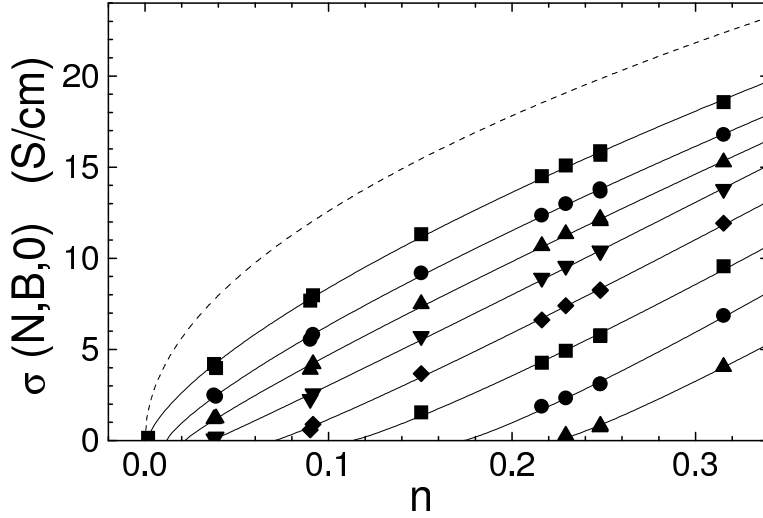


**Figure 11.** Zero-temperature conductivity  $\sigma(N, B, 0)$  vs normalized concentration  $n \equiv [\sigma(N, 0, 0)/\sigma^*(0)]^{2.0} = N/N_c(0) - 1$ , where  $\sigma(N, 0, 0)$  is the zero-temperature conductivity and  $\sigma^*(0)$  is the prefactor both at  $B = 0$ . From top to bottom the magnetic induction increases from 1 T to 8 T in steps of 1 T. The dashed curve at the top is for  $B = 0$ . The solid curves represent fits of  $\sigma(N, B, 0) \propto [n/n_c(B) - 1]^{\mu(B)}$ . For  $B \geq 6$  T, we assume  $\mu = 1.15$ .

where

$$m_B = \frac{e^2}{\hbar} \frac{1}{4\pi^2} \frac{1.3}{\sqrt{2}} \left( \frac{4}{3} - \frac{1}{2} \tilde{F} \right) \sqrt{\frac{k_B}{\hbar D}}. \quad (23)$$

One should note that Eqs. (9) and (22) are valid only in the limits of  $[\sigma(N, 0, T) - \sigma(N, 0, 0)] \ll \sigma(N, 0, 0)$  or  $[\sigma(N, B, T) - \sigma(N, B, 0)] \ll \sigma(N, B, 0)$ . It is for this reason that we have observed a  $T^{1/3}$  dependence rather than the  $\sqrt{T}$  dependence at  $B = 0$  in Fig. 2 as the critical point  $[\sigma(N, 0, 0) = 0]$  is approached from the metallic side. However, Fig. 10 shows that the  $\sqrt{T}$  dependence holds when  $B \neq 0$  even around the critical point. Hence, we use Eq. (22) to evaluate the zero-temperature conductivity  $\sigma(N, B, 0)$  in magnetic fields. Since  $m_B$  is independent of  $B$ , the conductivity for various values of  $B$  plotted against  $\sqrt{T}$  should appear as a group of parallel lines. This is approximately the case as seen in Fig. 10 at low temperatures (e.g.,  $T < 0.25$  K).

The zero-temperature conductivity  $\sigma(N, B, 0)$  in various magnetic fields obtained by extrapolation of  $\sigma(N, B, T)$  to  $T = 0$  based on Eq. (22) is shown in Fig. 11. Here,  $\sigma(N, B, 0)$  is plotted as a function of the normalized concentration:

$$n \equiv [\sigma(N, 0, 0)/\sigma^*(0)]^{2.0}. \quad (24)$$

Since the relation between  $N$  and  $\sigma(N, 0, 0)$  was established in Fig. 3(b) as  $\sigma(N, 0, 0) = \sigma^*(0)[N/N_c(0) - 1]^{0.50}$  where  $N_c(0) = 1.860 \times 10^{17} \text{ cm}^{-3}$  and  $\sigma^*(0) = 40 \text{ S/cm}$ ,  $n$  is equivalent to  $N/N_c(0) - 1$ . Henceforth, we will use  $n$  instead of  $N$  because employing  $n$  reduces the scattering of the data caused by several experimental uncertainties, and it further helps us concentrate on observing how  $\sigma(N, B, 0)$  varies as  $B$  is increased. Similar evaluations of the concentration have been used by various groups. In their approach, the ratio of the resistance at 4.2 K to that at a room temperature is used to determine the concentration [5]. The dashed curve in Fig. 11 is for  $B = 0$ , which merely expresses Eq. (24), and the solid curves represent fits of

$$\sigma(N, B, 0) = \sigma_0(B)[n/n_c(B) - 1]^{\mu(B)}. \quad (25)$$

The exponent  $\mu(B)$  increases from 0.5 with increasing  $B$  and reaches a value close to unity at  $B \geq 4$  T. For example,  $\mu = 1.03 \pm 0.03$  at  $B = 4$  T and  $\mu = 1.09 \pm 0.05$  at

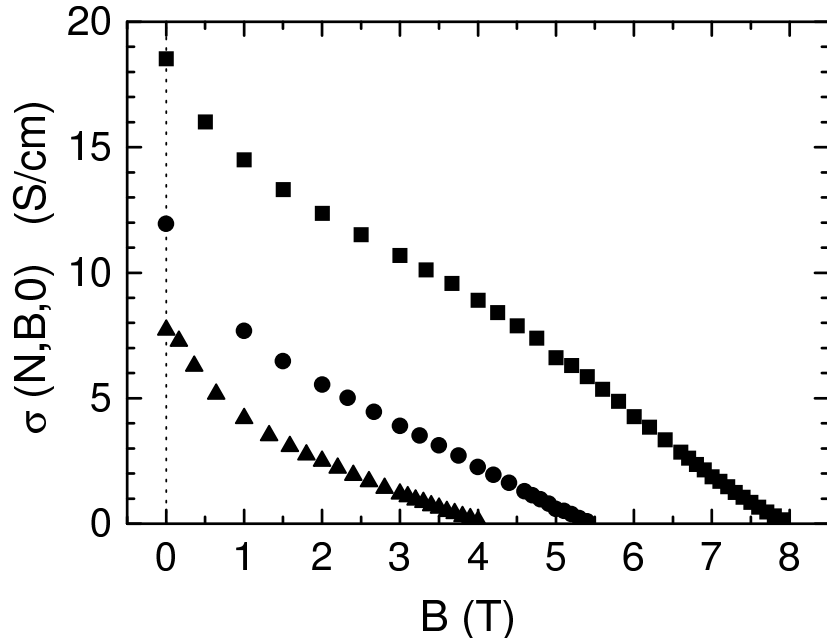


**Figure 12.** Zero-temperature conductivity  $\sigma(N, B, 0)$  vs magnetic induction  $B$ . From bottom to top, the normalized concentrations defined by Eq. (24) are 0.04, 0.09, and 0.22, respectively.

$B = 5$  T. When  $B \geq 6$  T, three-parameter  $[\sigma_0(B), n_c(B), \text{ and } \mu(B)]$  fits no longer give reasonable results because the number of samples available for the fit decreases with increasing  $B$ . Hence, we give the solid curves for  $B \geq 6$  T assuming  $\mu(B) = 1.15$ .

We show  $\sigma(N, B, 0)$  as a function of  $B$  in Fig. 12 for three different samples. When the magnetic field is weak, i.e., the correction  $\Delta\sigma_B(N, B, 0) \equiv \sigma(N, B, 0) - \sigma(N, 0, 0)$  due to  $B$  is small compared with  $\sigma(N, 0, 0)$ , the field dependence of  $\Delta\sigma_B(N, B, 0)$  looks consistent with the prediction by the interaction theory [1],

$$\Delta\sigma_B(N, B, 0) = -\frac{e^2}{\hbar} \frac{\tilde{F}}{4\pi^2} \sqrt{\frac{g\mu_B B}{2\hbar D}} \propto \sqrt{B}. \quad (26)$$

In larger magnetic fields,  $\sigma(N, B, 0)$  deviates from Eq. (26) and eventually vanishes at some magnetic induction  $B_c$ . For the samples in Fig. 12, we tuned the magnetic induction to the MIT in a resolution of 0.1 T. We fit an equation similar to Eq. (25),

$$\sigma(N, B, 0) = \sigma'_0(n)[1 - B/B_c(n)]^{\mu'(n)}, \quad (27)$$

to the data close to the critical point. As a result we obtain  $\mu' = 1.1 \pm 0.1$  for all of the three samples. The value of  $\mu'$  depends on the choice of the magnetic-field range to be used for the fitting, and this fact leads to the error of  $\pm 0.1$  in the determination of  $\mu'$ . In Fig. 13 we show that  $\mu' = 1.1$  yields an excellent finite-temperature scaling [Eq. (3)]. Note that the data both on the metallic side and on the insulating side are included in this scaling plot. Here we employ  $B_c$  obtained by fitting Eq. (27),  $x = 1/2$  from the fact that  $\sqrt{T}$  dependence holds in magnetic fields even around the critical point, and  $y = x/\mu' = 0.45$ , i.e., none of them are treated as a fitting parameter. Hence, Fig. 13 strongly supports  $\mu' = 1.1$ .

From the critical points  $n_c(B)$  and  $B_c(n)$ , the phase diagram at  $T = 0$  is constructed on the  $(N, B)$  plane as shown in Fig. 14. Here,  $n_c(B)$  for  $B \geq 6$  T shown by triangles are obtained by assuming  $\mu = 1.15$ . The vertical solid lines associated with the triangles represent the range of values over which  $n_c(B)$  have to exist, i.e., between the highest  $n$  in the insulating phase and the lowest  $n$  in the metallic phase. Solid diamonds

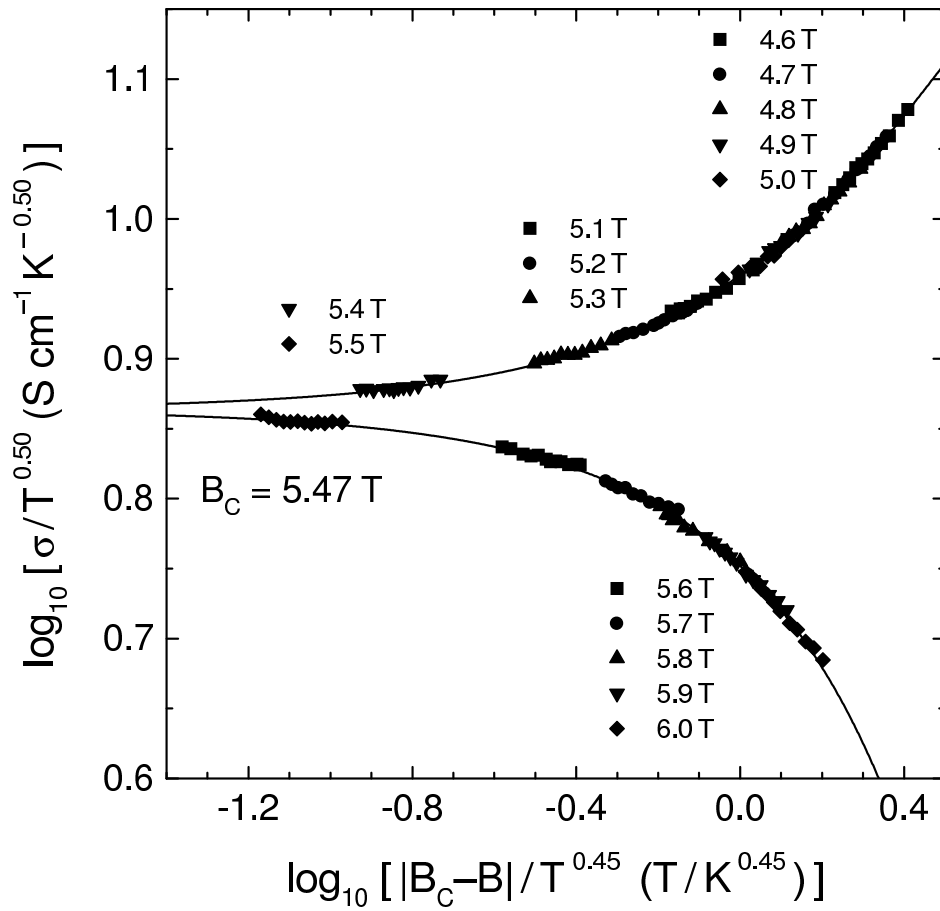


**Figure 13.** Finite-temperature scaling plot for the field-induced metal-insulator transition in the  $^{70}\text{Ge}:\text{Ga}$  sample having  $n = 0.09$ .

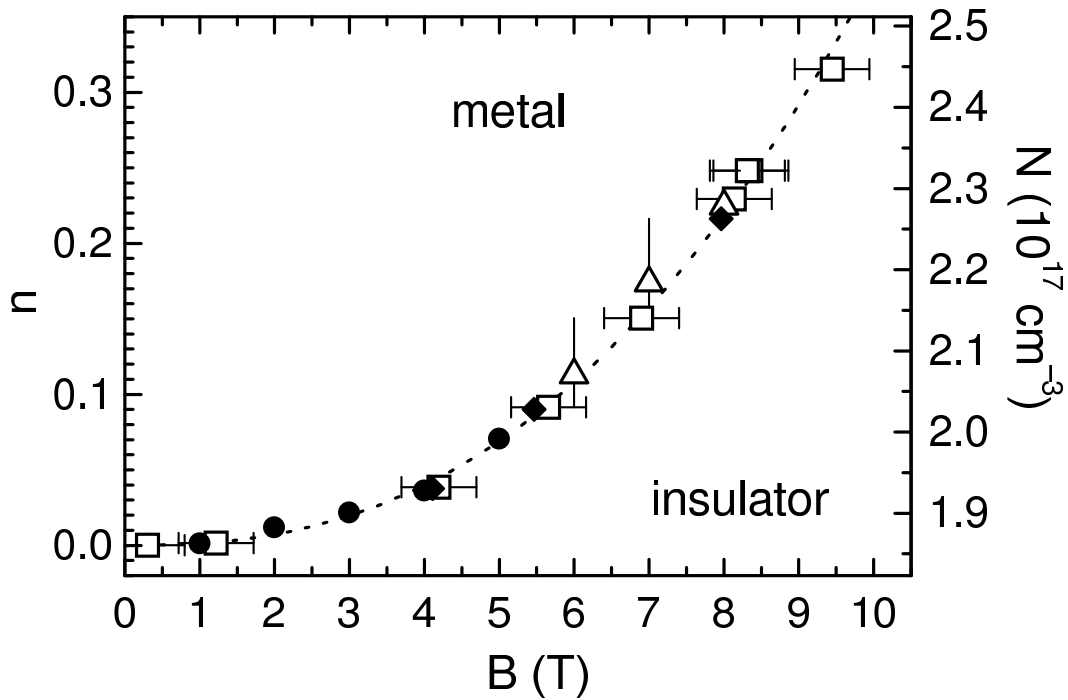


**Figure 14.** Phase diagram of  $^{70}\text{Ge}:\text{Ga}$  at  $T = 0$ . The solid circles and the open triangles represent the critical concentrations  $n_c$ , and the solid diamonds and the open boxes represent the critical magnetic induction  $B_c$ .

represent  $B_c$  for the three samples in which we have studied the magnetic-field-induced MIT. Estimations of  $B_c$  for the other samples are also shown by open boxes with error bars. The boundary between metallic phase and insulating phase is expressed by a power-law relation:

$$n = C_3 B^\beta. \quad (28)$$

From the eight data points denoted by the solid symbols, we obtain  $C_3 = (1.33 \pm 0.17) \times 10^{-3} \text{ T}^{-\beta}$  and  $\beta = 2.45 \pm 0.09$  as shown by the dotted curve. The shift of  $N_c$  in magnetic fields was studied theoretically by Khmel'nitskii and Larkin [29]. They considered a noninteracting electron system starting from

$$\sigma(N, B, 0) \approx \frac{e^2}{\hbar \xi'} f_2(B^{\alpha'} \xi'), \quad (29)$$

where  $\xi'$  is the correlation length. They claimed that the argument of the function  $f_2$  should be a power of the magnetic flux through a region with dimension  $\xi'$ . This means

$$\sigma(N, B, 0) \approx \frac{e^2}{\hbar \xi'} f_2(\xi'/\lambda), \quad (30)$$

where  $\lambda \equiv \sqrt{\hbar/eB}$  is the magnetic length, and hence,  $\alpha' = 1/2$ . In order to discuss the shift of the MIT due to the magnetic field, they rewrote Eq. (30) as

$$\sigma(N, B, 0) \approx \frac{e^2}{\hbar \lambda} \phi(t \lambda^{1/\nu}), \quad (31)$$

based on the relation in zero magnetic field

$$\xi' \propto t^{-\nu}. \quad (32)$$

Here,  $t$  is a measure of distance from the critical point in zero field, e.g.,

$$t \equiv [N/N_c(0) - 1]. \quad (33)$$

The zero point of the function  $\phi$  gives the MIT, and the shift of the critical point for the MIT equals

$$N_c(B) - N_c(0) \propto B^{1/2\nu}. \quad (34)$$

Thus,  $\beta = 1/(2\nu)$  results. In the present system, however, this relation does not hold, as long as we assume  $\mu = \nu$  [3]. Experimentally, we find  $\beta = 2.5$ , while  $1/(2\nu) = 1/(2\mu) = 1$  for  $^{70}\text{Ge}:\text{Ga}$  at  $B = 0$ .

Based on the phase diagram we shall consider the relationship between the two critical exponents:  $\mu$  for the doping-induced MIT and  $\mu'$  for the magnetic-field-induced MIT. Suppose that a sample with normalized concentration  $n$  has a zero-temperature conductivity  $\sigma$  at  $B \neq 0$  and that  $[n/n_c(B) - 1] \ll 1$  or  $[1 - B/B_c(n)] \ll 1$ . From Eqs. (25) and (27), we have two expressions for  $\sigma$ :

$$\sigma = \sigma_0 (n/n_c - 1)^\mu \quad (35)$$

and

$$\sigma = \sigma'_0 (1 - B/B_c)^{\mu'}. \quad (36)$$

On the other hand, we have from Eq. (28)

$$n/n_c = (B/B_c)^{-\beta} = [1 - (1 - B/B_c)]^{-\beta} \approx 1 + \beta(1 - B/B_c) \quad (37)$$

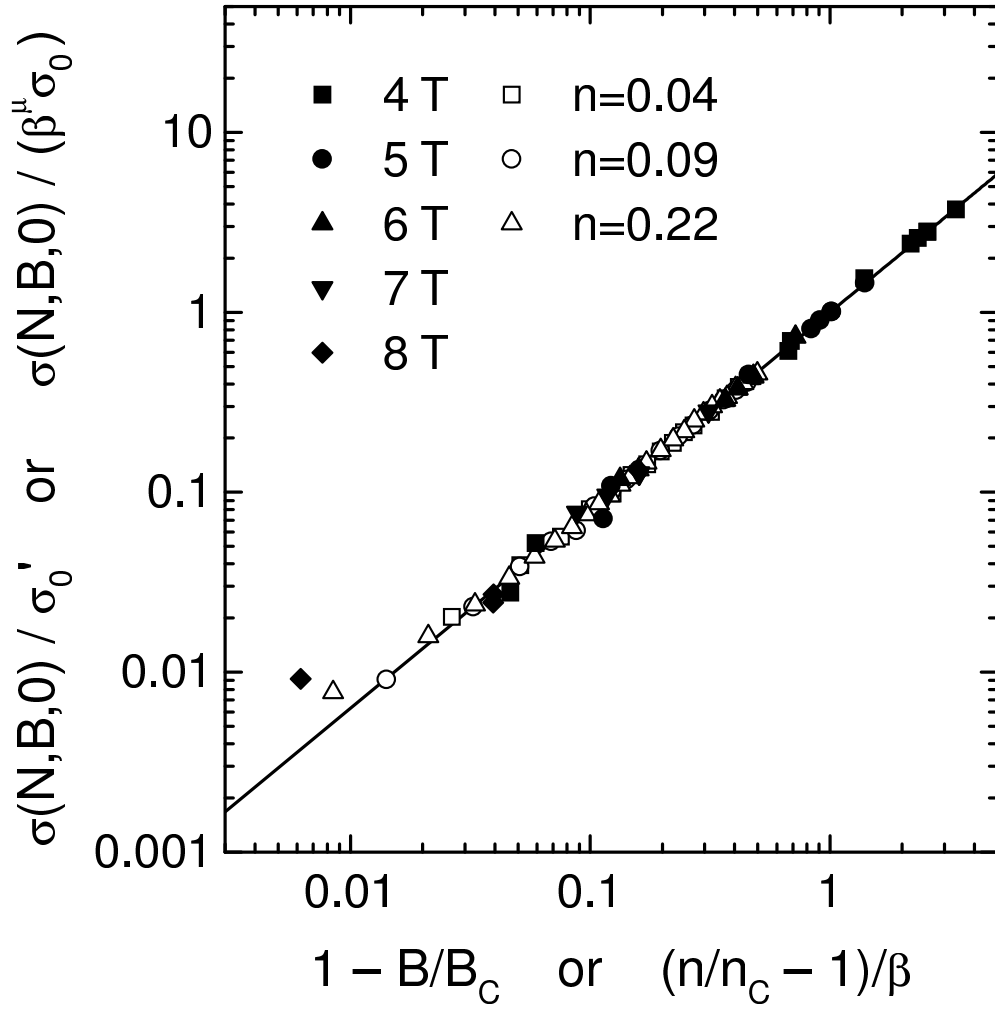


**Figure 15.** Normalized zero-temperature conductivity  $\sigma(N, B, 0)/\sigma'_0(n)$  and  $\sigma(N, B, 0)/[\beta^\mu \sigma_0(B)]$  as functions of  $[1 - B/B_c(n)]$  and  $[n/n_c(B) - 1]/\beta$ , respectively, where  $\beta = 2.5$  and  $\mu = 1.1$ . The solid line denotes a power-law behavior with the exponent of 1.1. The open and solid symbols represent the results of the magnetic-field-induced metal-insulator transition (MIT) in the range  $(1 - B/B_c) < 0.5$  for three different samples ( $n = 0.04, 0.09$ , and  $0.22$ ) and the doping-induced MIT in constant magnetic fields (4, 5, 6, 7, and 8 T), respectively.

in the limit of  $(1 - B/B_c) \ll 1$ . This equation can be rewritten as

$$(n/n_c - 1)/\beta \approx (1 - B/B_c). \quad (38)$$

Using Eqs. (35), (36), and (38), we obtain

$$\sigma'_0(1 - B/B_c)^{\mu'} \approx \beta^\mu \sigma_0(1 - B/B_c)^\mu. \quad (39)$$

Since Eq. (39) has to hold for arbitrary  $B$ , the following relations

$$\sigma'_0 = \beta^\mu \sigma_0 \quad (40)$$

and

$$\mu' = \mu \quad (41)$$

are derived.

In Fig. 15 we see how well Eq. (41) holds for the present system. We have already shown in Fig. 12 that  $\mu' = 1.1 \pm 0.1$  is practically independent of  $n$ . Concerning the

exponent  $\mu$ , however, its dependence on  $B$  has not been ruled out completely even for the highest  $B$  we used in the experiments. This is mainly because the number of available data points at large  $B$  is not sufficient for a precise determination of  $\mu$ . In Fig. 15 the results of the doping-induced MIT for  $B \geq 4$  T (solid symbols) and the magnetic-field-induced MIT for three different samples (open symbols) are plotted. Here, we plot  $\sigma(N, B, 0)/[\beta^\mu \sigma_0(B)]$  vs  $[n/n_c(B) - 1]/\beta$  with  $\beta = 2.5$  and  $\mu = 1.1$  for the doping-induced MIT, and  $\sigma(N, B, 0)/\sigma_0(B)'$  vs  $[1 - B/B_c(n)]$  for the magnetic-field-induced MIT. Figure 15 shows that the data points align exceptionally well along a single line describing a single exponent  $\mu = \mu' = 1.1$ .

We saw in Fig. 11 that  $\mu$  apparently takes smaller values in  $B \leq 3$  T, which seemingly contradicts the above consideration. We can understand this as follows. We find that the critical exponent  $\mu$  in zero magnetic field is 0.5 which is different from the values of  $\mu$  in magnetic fields. Hence, one should note whether the system under consideration belongs to the “magnetic-field regime” or not. In systems where the MIT occurs, there are several characteristic length scales: the correlation length, the thermal diffusion length, the inelastic scattering length, the spin scattering length, the spin-orbit scattering length, etc. As for the magnetic field, it is characterized by the magnetic length  $\lambda \equiv \sqrt{\hbar/eB}$ . When  $\lambda$  is smaller than the other length scales, the system is in the “magnetic-field regime.” As the correlation length  $\xi'$  diverges at the MIT,  $\lambda < \xi'$  holds near the critical point, no matter how weak the magnetic field is. When the field is not sufficiently large, the “magnetic-field regime” where we assume  $\mu = 1.1$  to hold, is restricted to a narrow region of concentration. Outside the region, the system crosses over to the “zero-field regime” where  $\mu = 0.5$  is expected. This is what is seen in Fig. 11.

## CONCLUSION

We have measured the electrical conductivity of NTD  $^{70}\text{Ge}:\text{Ga}$  to study the metal-insulator transition, ruling out an ambiguity due to inhomogeneous distribution of impurities. The critical exponent  $\mu \approx 0.5$  in zero magnetic field for doped semiconductors without impurity compensation has been confirmed. On the insulating side of the MIT, while the relation  $2\nu \approx \zeta$  predicted by scaling theories [15] holds for  $0.9 < N/N_c < 1$ , the critical exponents for localization length and impurity dielectric susceptibility change at  $N/N_c \approx 0.99$ . The small amount of doping compensation that is unavoidably present in our samples may be responsible for such a change in the exponents. We have also measured the conductivity in magnetic fields up to  $B = 8$  T in order to study the doping-induced MIT (in magnetic fields) and the magnetic-field-induced MIT. For both of the MIT, the critical exponent of the conductivity is 1.1, which is different from the value 0.5 at  $B = 0$ . The change of the critical exponent caused by the applied magnetic fields supports a picture in which  $\mu$  varies depending on the universality class to which the system belongs. The phase diagram has been determined in magnetic fields for the  $^{70}\text{Ge}:\text{Ga}$  system.

## ACKNOWLEDGMENTS

This work has been performed in collaboration with K. M. Itoh, Y. Ootuka, and E. E. Haller. We are thankful to T. Ohtsuki for fruitful discussions, and to S. Katsumoto, B. I. Shklovskii, M. P. Sarachik, and J. C. Phillips for valuable comments. The author is supported by Research Fellowship of Japan Society for the Promotion of Science for Young Scientists.

## REFERENCES

1. Lee, P.A. and Ramakrishnan, T.V. (1985) Disordered electronic systems, *Rev. Mod. Phys.* **57**, 287-337.
2. Belitz, D. and Kirkpatrick, T.R. (1994) The Anderson-Mott transition, *Rev. Mod. Phys.* **66**, 261-380.
3. Wegner, F.J. (1976) Electrons in disordered systems. Scaling near the mobility edge, *Z. Phys. B* **25**, 327-337; (1979) The mobility edge problem: continuous symmetry and a conjecture, *ibid.* **35**, 207-210.
4. Rosenbaum, T.F. Milligan, R.F. Paalanen, M.A. Thomas, G.A. Bhatt, R.N. and Lin, W. (1983) Metal-insulator transition in a doped semiconductor, *Phys. Rev. B* **27**, 7509-7523.
5. Stupp, H. Hornung, M. Lakner, M. Madel, O. and Löhneysen, H.v. (1993) Possible solution of the conductivity critical exponent puzzle for the metal-insulator transition in heavily doped uncompensated semiconductors, *Phys. Rev. Lett.* **71**, 2634-2637.
6. Waffenschmidt, S. Pfeleiderer, C. and Löhneysen, H.v. (1999) Critical behavior of the conductivity of Si:P at the metal-insulator transition under uniaxial stress, *Phys. Rev. Lett.* **83**, 3005-3008.
7. Rosenbaum, T.F. Thomas, G.A. and Paalanen, M.A. (1994) Critical behavior of Si:P at the metal-insulator transition, *Phys. Rev. Lett.* **72**, 2121.
8. Zulehner, W. (1989) Czochralski growth of silicon, in Harbeke, G. and Schulz, M.J. (eds.) *Semiconductor Silicon: Material Science and Technology*, Springer-Verlag, Berlin, pp. 2-23.
9. Haller, E.E. Palaio, N.P. Rodder, M. Hansen, W.L. and Kreysa, E. (1984) NTD germanium: a novel material for low temperature bolometers, in Larrabee, R.D. (ed.) *Neutron Transmutation Doping of Semiconductor Materials*, Plenum, New York, pp. 21-36.
10. Itoh, K.M. Haller, E.E. Beeman, J.W. Hansen, W.L. Emes, J. Reichertz, L.A. Kreysa, E. Shutt, T. Cummings, A. Stockwell, W. Sadoulet, B. Muto, J. Farmer, J.W. and Ozhogin, V.I. (1996) Hopping conduction and metal-insulator transition in isotopically enriched neutron-transmutation-doped  $^{70}\text{Ge}:\text{Ga}$ , *Phys. Rev. Lett.* **77**, 4058-4061.
11. Watanabe, M. Ootuka, Y. Itoh, K.M. and Haller, E.E. (1998) Electrical properties of isotopically enriched neutron-transmutation-doped  $^{70}\text{Ge}:\text{Ga}$  near the metal-insulator transition, *Phys. Rev. B* **58**, 9851-9857.
12. Watanabe, M. Itoh, K.M. Ootuka, Y. and Haller, E.E. (2000) Localization length and impurity dielectric susceptibility in the critical regime of the metal-insulator transition in homogeneously doped *p*-type Ge, *Phys. Rev. B* **62**, R2255-R2258.
13. Shklovskii, B.I. and Efros, A.L. (1984) *Electronic Properties of Doped Semiconductors*, Springer-Verlag, Berlin.
14. Ionov, A.N. Shlimak I.S. and Matveev, M.N. (1983) An experimental determination of the critical exponents at the metal-insulator transition, *Solid State Commun.* **47**, 763-766.
15. Kawabata, A. (1984) Renormalization group theory of metal-insulator transition in doped silicon, *J. Phys. Soc. Jpn.* **53**, 318-323.
16. Hess, H.F. DeConde, K. Rosenbaum, T.F. and Thomas, G.A. (1982) Giant dielectric constants at the approach to the insulator-metal transition, *Phys. Rev. B* **25**, 5578-5580.
17. Katsumoto, S. (1990) Photo-induced metal-insulator transition in a semiconductor, in Kuchar, F. Heinrich, H. and Bauer, G. (eds.) *Localization and Confinement of Electrons in Semiconductors*, Springer-Verlag, Berlin, pp. 117-126.
18. Chayes, J.T. Chayes, L. Fisher, D.S. and Spencer, T. (1986) Finite-size scaling and correlation lengths for disordered systems, *Phys. Rev. Lett.* **57**, 2999-3002.
19. Kirkpatrick, T.R. and Belitz, D. (1993) Logarithmic corrections to scaling near the metal-insulator transition, *Phys. Rev. Lett.* **70**, 974-977.
20. Watanabe, M. Itoh, K.M. Ootuka, Y. and Haller, E.E. (1999) Metal-insulator transition of isotopically enriched neutron-transmutation-doped  $^{70}\text{Ge}:\text{Ga}$  in magnetic fields, *Phys. Rev. B* **62**, 15817-15823.
21. Al'tshuler, B.L. and Aronov, A.G. (1983) Scaling theory of Anderson's transition for interacting electrons, *JETP Lett.* **37**, 410-413.
22. Ohtsuki, T. and Kawarabayashi, T. (1997) Anomalous diffusion at the Anderson transitions, *J. Phys. Soc. Jpn.* **66**, 314-317.
23. Abrahams, E. Anderson, P.W. Licciardello, D.C. and Ramakrishnan, T.V. (1979) Scaling theory of localization: absence of quantum diffusion in two dimensions, *Phys. Rev. Lett.* **42**, 673-676.
24. Bernreuther, W. and Wegner, F.J. (1986) Four-loop-order  $\beta$  function for two-dimensional nonlinear sigma models, *Phys. Rev. Lett.* **57**, 1383-1385.

25. Castner, T.G. Lee, N.K. Tan, H.S. Moberly, L. and Symko O. (1980) The low-frequency, low-temperature dielectric behavior of *n*-type germanium below the insulator-metal transition, *J. Low Temp. Phys.* **38**, 447-473.
26. Bhatt, R.N. and Rice, T.M. (1980) Clustering in the approach to the metal-insulator transition, *Philos. Mag. B* **42**, 859-872.
27. Rentzsch, R. Ionov, A.N. Reich, Ch. Müller, M. Sandow, B. Fozooni, P. Lea, M.J. Ginodman, V. and Shlimak, I. (1998) The scaling behaviour of the metal-insulator transition of isotopically engineered neutron-transmutation doped germanium, *Phys. Status Solidi B* **205**, 269-273.
28. Itoh, K.M. Watanabe, M. Ootuka, Y. and Haller, E.E. (1999) Scaling analysis of the low temperature conductivity in neutron-transmutation-doped <sup>70</sup>Ge:Ga, *Ann. Phys. (Leipzig)* **8**, 631-637.
29. Khmel'nitskii, D.E. and Larkin, A.I. (1981) Mobility edge shift in external magnetic field, *Solid State Commun.* **39**, 1069-1070.